Chapter

Coherent Doppler Lidar for Wind Sensing

Sameh Abdelazim, David Santoro, Mark F. Arend, Fred Moshary and Sam Ahmed

Abstract

An eye-safe all-fiber Coherent Doppler Lidar for wind sensing system has been developed and tested at the Remote Sensing Laboratory of the City College of New York, New York, NY. The system, which operates at a 20 kHz pulse repetition rate and acquires lidar return signals at 400 MSample/s, accumulates signals that are as much as 20 dB lower than the receiver noise power by using embedded programming techniques. Two FPGA embedded programming algorithms are designed and compared. In the first algorithm, power spectra of return signals are calculated and accumulated for different range gates. Line of sight wind speed estimates can then be calculated after transferring the range gated accumulated power spectra to a host computer. In the second FPGA algorithm, a digital IQ demodulator and down sampler allow an autocorrelation matrix representing a pre-selected number of lags to be accumulated. Precision in the velocity measurements is estimated to be on the order of 0.08 m/s and the precision in the measured horizontal wind direction is estimated to be to be about 2°.

Keywords: Doppler Lidar, wind sensing, heterodyne detection, FPGA, coherent laser, eye-safe

1. Introduction

The first wind measurement device (anemometer) was invented in 1450 by an Italian architect named Leon Battista Alberti. Four hemispherical cups anemometer was later invented in 1846 by Dr. John Thomas Romney Robinson. Today, wind speed and direction can be measured by using classical anemometers, sonic anemometers, rawinsondes, SODAR (Sonic Detection and Ranging), RADAR (Radio Detection and Ranging), and LIDAR (Light Detection and Ranging). Sonic anemometers determines instantaneous wind speed and direction by measuring how much sound waves traveling between a pair of transducers are sped up or slowed down by the effect of wind. SODAR measures wind speed through measurements of the scattering of sound waves by atmospheric turbulence. Both radar and LIDAR use similar technique such as SODAR but instead of using sound waves, radar uses microwave, and LIDAR uses laser waves.

Sodars and radars are used in wind profilers to measure wind speed and direction at various altitudes above ground level. Wind speed can be estimated by transmitting five beams; one is vertical to measure vertical wind velocity, and the other beams are orthogonal to each other to measure horizontal components of the wind. The profiler's assumption to measure wind speed is that turbulent eddies that

scatter probing signals are carried along by the mean wind. **Figure 1** shows radar and sodar wind profilers that are mounted at Liberty Science Center, New Jersey, and on top of the Metlife building in the center of Manhattan, New York, respectively, as part of the New York City meteorological network (NYC MetNet). These types of instruments are large and not portable.

Coherent Doppler Lidar (CDL) has proven to be a powerful tool for remote sensing of the atmosphere, and has been widely adopted in applications such as measuring atmospheric wind velocity, turbulence, aerosol concentration, cloud height and velocity, and detection of atmospheric constituents and pollutants. The CDL systems have been developed for remote sensing measurements since the late 1960's. The first CDL wind-sensing system was reported by Huffaker et al. [1], where a 10.6 μm cw CO_2 laser was used. CO_2-laser-based CDL systems have been used for airborne clear air wind and hard target measurements such as ranging and produced valuable results for a long time. Since the late 1980s, CDL systems with newly developed solid-state lasers attracted a lot of researchers due to advantages of size, weight, reliability, and lifetime [2].

Operation at shorter wavelengths allows for higher spectral resolution, which means higher velocity resolution. A lot of effort has been put into 2 μm pulsed systems mainly intended for wind measurements [3–5]. Kavaya et al. [6] developed a 1.06 μm pulsed CDL system that realized a measurable range of a few tens of kilometers used for launch-site wind sensing. Karlsson et al. [3] reported a 1.5 μm cw all-fiber wind sensing CDL system, which utilized optical fiber components used in telecommunication systems.

In this study, we report on the design, measurements, and performance of a CDL system for wind measurements [7]. The design involves a very low energy per pulse (12 μJ/pulse), because it employs all-fiber optic laser components for availability, cost affordability, robustness, and size compactness. As a result of this low energy per pulse, a very high frequency repetition rate (FRP) is used, which produces a very large volume of returned signals. Acquiring such a large volume of data at a very high sampling rate and processing it cannot be achieved using a classical data acquisition and processing hardware. Therefore, signal pre-processing has to be carried out on hardware level by means of the FPGA, which allows for real time processing and a moderate data transfer rate from the data acquisition card to the host PC. In our design, signal pre-processing was implemented to produce the power spectrum of time gated received signals by calculating fast Fourier transform FFT, which produces fixed spatial resolution gates. Another pre-processing technique was implemented that involved the calculation of received signals' autocorrelation, which can be used to find the power spectrum at any desired range resolution.

The system consists of a distributed-feedback (DFB) semiconductor laser emitting at a 1.5 μm in addition to an erbium-doped fiber amplifier (EDFA) in a master

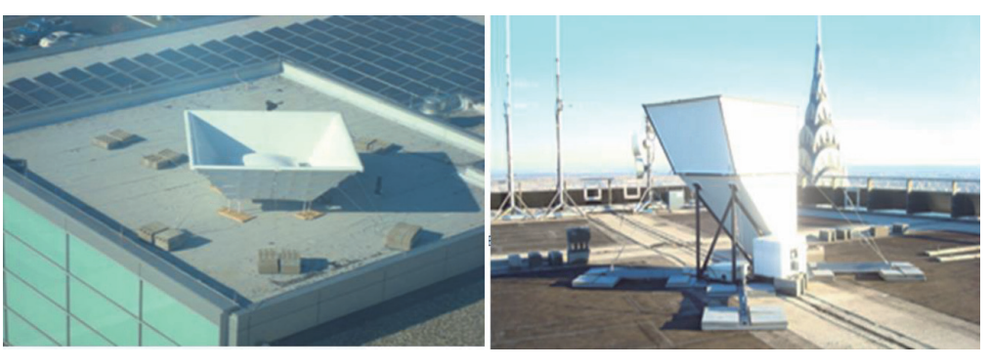

Figure 1.
A radar wind profiler (left) mounted on the liberty science center and a sodar wind profiler (right) mounted on a NYC high rise [8].

oscillator power amplifier (MOPA) configuration. A notable feature of our system is that it utilizes polarized maintained (PM) fiber optics, which ensures the maintaining of polarization state between both local oscillator and back scattered fields. The advantage of using a 1.5 μm laser source is the eye-safety feature, which allows for operation in urban areas. In addition to eye-safety feature, the usage of a 1.5 μm source allows the system to benefit from the technology and component development driven by the telecommunication industry, which results in significant cost deductions.

In this study, the development and operation of a CDL system for wind sensing is presented. In Section 2, the system configuration is presented and system's main components are described. In Section 3, transceiver noise analysis and coherent lidar signal range dependence are examined. In Section 4, signal processing and FPGA programming is introduced. In Section 5, wind measurement results are reported in both vertical pointing and scan modes.

1.1 Coherent Doppler lidar theory

In coherent Doppler lidar, laser pulses are transmitted into the atmosphere and interact with aerosols within the atmosphere. As a result of this interaction, laser signals are backscattered towards the laser source, which can be detected and measured through an optical detector. According to the movement of the atmospheric aerosols with respect to the laser source, backscattered signals may suffer a frequency shift (Doppler shift) that is proportional to velocity of moving aerosols. The Doppler shift Δf of laser signals with λ wave length is given by:

$$\Delta f = \frac{2\nu}{\lambda} \tag{1}$$

where ν is the velocity of the aerosols, i.e. wind velocity.

1.2 Heterodyne detection theory

In heterodyne optical detection, local oscillator and backscattered signals are optically mixed through an optical coupler. The resulting mixed signal is then incident upon a photodetector. Both local oscillator and backscattered fields can be represented as:

$$x_{lo} = A_{lo}\, cos\,(\omega_o t) \tag{2}$$

$$x_s = A_s\, cos\,(\omega_o t + \omega_s t) \tag{3}$$

where ω_0 is the local oscillator frequency and ω_s is the frequency shift that backscattered signals may suffer. The optical intensity as seen by the heterodyne detector is given by:

$$\begin{aligned} I_{opt} &= [A_{lo}\cos(\omega_o t) + A_s \cos(\omega_o t + \omega_s t)]^2 \\ &= \frac{{A_{lo}}^2}{2} + \frac{{A_s}^2}{2} + A_{LO}A_s \cos(\omega_s t) + (\text{High frequency component}) \end{aligned} \tag{4}$$

The terms: $2\omega_0$, $2(\omega_0 + \omega_s)$, and $(2\omega_0 + \omega_s)$ are at higher frequencies than detector's bandwidth and will not be seen by the detector. As a result, the generated photodiode electric current will equal to:

$$I_d = \eta A I_{opt} \tag{5}$$

$$= \frac{\eta A {A_{lo}}^2}{2} + \frac{\eta A {A_s}^2}{2} + \eta A A_{lo} A_s \cos(\omega_s t) \quad (6)$$

$$= \eta P_{lo} + \eta P_s + 2\eta\sqrt{P_{lo}P_s}\cos(\omega_s t) \quad (7)$$

where: A and η are detector's surface area and photo responsivity, respectively. I_d consists of a dc component = ηP_{lo} + ηP_s and an ac component = $2\eta\sqrt{P_{lo}P_s}\cos(\omega_s t)$. since $P_{lo} >> P_s$, then:

$$I_{d(dc)} = \eta P_{lo} \quad (8)$$

$$I_{d(ac)} = 2\eta\sqrt{P_{lo}P_s}\cos(\omega_s t) \quad (9)$$

Signal power can be calculated as:

$$< i_s^2 > = \left(I_{d(rms)}\right)^2 \quad (10)$$

$$= 2\eta^2 P_{lo} P_s \quad (11)$$

Detector's responsivity is related to detector's quantum efficiency through the following relationship:

$$\eta = \frac{e\eta_q}{h\upsilon} \quad (12)$$

where; e is electron charge, η_q is the quantum efficiency of the detector, h is Plank's constant, ν is laser's frequency,

$$< i_s^2 > = 2\left(\frac{e\eta_q}{h\upsilon}\right)^2 P_{lo} P_s \quad (13)$$

In this system, backscattered signals are sampled at 400 MHz using a 14-bit ADC equipped with an on-board FPGA. The laser pulse frequency rate (PFR) is 20 kHz, which limits the maximum measurement range to 7.5 km. To estimate wind velocity, the frequency shift of scattered signals (Doppler shift) has to be extracted. Backscattered signals are broken into time gates to represent desired range distances and a power spectrum of each range gate is calculated by Fast Fourier Transform (FFT). A gate length of 128 data samples is chosen, which corresponds to 48 m range distance. Due to low pulse energy (14 μJ/pulse), power spectrum accumulation is needed to improve detection probability and velocity estimation accuracy. The wind velocity of each range gate is estimated from the calculated mean frequency of a post processed power spectrum around the peak frequency.

2. SYSTEM'S configurations

In this section, the main system components are presented and an over view of the system's operation is explained. System's configurations and testing of optical and electrical components are also presented in this section.

2.1 System overview

The system configuration is shown in **Figure 2**, which consists of the following components: (i) Laser source (ii) Accousto-optic modulator (iii) Fiber amplifier (iv) Optical circulator (v) Optical antenna (vi) Balanced detector, and (vii) Signal

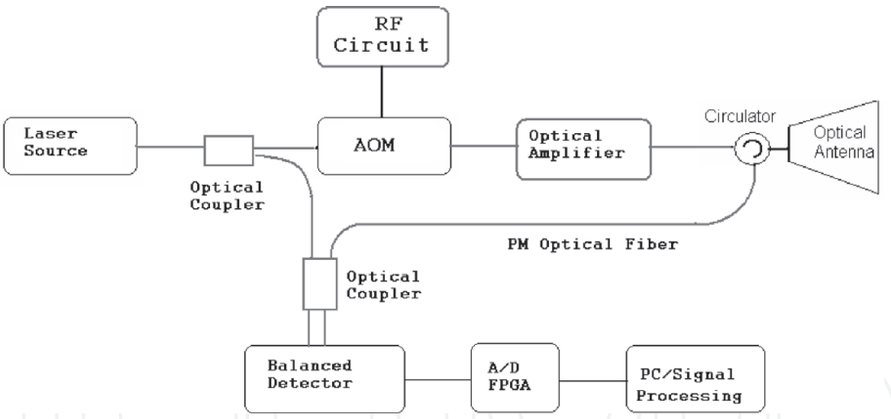

Figure 2.
Coherent Doppler Lidar system's configuration.

processor. Optical components are connected with a single mode polarized maintained (PM) optical fiber.

Our laser source has two outputs: a low power seed laser that is used as a local oscillator (LO), and a high power output (0.5 W) that is modulated, pulsed, and frequency shifted using an acousto-optic modulator (AOM). Electronic circuits drive the AOM to shift laser signals by 84 MHz and generate 200 ns Gaussian shaped laser pulses. These laser pulses are amplified through an erbium doped fiber amplifier (EDFA) then transmitted from port 1 to port 2 of the optical circulator. To minimize the back reflection from port 2 back to port 1, the fiber tip at port 2 is angled and polished. Laser pulses are transmitted into the atmosphere and aerosol particles scatter the laser signals back into the lens, which in turn are transmitted from the optical circulator's port 2 to port 3. Backscattered and LO signals are optically mixed using an optical coupler. Optically mixed signals are heterodyne detected through an optical balanced detector, which generates RF signals. These RF signals are acquired at a 400 MHz sampling rate using an analog to digital converter card (ADC), which is equipped with an on-board field programmable gate array (FPGA) to allow for real time analysis. Digital data is then streamed to a host PC for further processing. More detailed explanations of key components are presented below.

2.2 Laser source

The laser source is a distributed feedback erbium doped fiber laser (DFB-EDFL) from NP Photonics. The laser's wavelength is 1545.2 nm, and it has two outputs; first output, used as a seed laser, and second output has an adjustable output power up to 500 mW. The spectrum of the delayed heterodyne detected signal as measured by a spectrum analyzer has a full width at half-maximum (FWHM) of a few kHz. The laser linewidth is approximately 3 kHz, which corresponds to a velocity estimation accuracy of 0.2 cm s^{-1}, so the laser linewidth is enough for our specification.

2.3 AOM

The continuous wave (CW) laser input is frequency shifted and pulsed through the AOMs, where an ultrasonic pulse is generated at a piezoelectric device by driving RF signals. Two AOMs are connected in series to obtain a very low extinction ratio. Each AOM shifts the frequency by 42 MHz, which leads to a total frequency shift of 84 MHz. The purpose of shifting the frequency of transmitted signals by 84 MHz is to shift the frequency of the zero velocity, so that both positive and negative Doppler shifts could be recognized. The driving RF signals, turn the

AOMs on during the 300 ns of the 20 kHz RF driving pulse to generate a laser pulse with 200 ns Full Width at Half Maximum (FWHM).

2.4 Fiber amplifier

An erbium-doped fiber amplifier (EDFA) that has an average power of 340 mW and a peak power of 74.6 W is used. This peak value cannot be increased beyond 74.6 W because of the Stimulated Brillouin Scattering (SBS), which can take place when an intense laser beam travels through a medium such as an optical fiber. SBS is generated from the acoustic vibrations in the medium that are caused by variations of the electric field of a traveling laser beam. Usually a laser beam undergoes SBS in an opposite direction to the incoming beam, which in our case can go back to the laser amplifier and cause damage to it. The EDFA has two amplifier stages; preamplifier and power amplifier. Output power is adjusted in a current control mode by adjusting the current of the power amplifier stage.

2.5 Optical circulator

The optical circulator ensures that the amplified output laser pulse is transmitted into the optical antenna and not into the detector. It also ensures that received backscattered signals and signals reflected off the fiber tip from the output pulse are directed into the receiver and not into the fiber amplifier. The back-reflection signal level at the fiber tip of the output port (port 2) of the optical circulator is very critical, because it can damage the optical detector.

2.6 Optical antenna

A 4″ diameter lens with a focal length of 50 cm is used. The truncation ratio is approximately 0.88, and the lens' Rayleigh range is approximately 5 km, which means that the laser beam can be collimated for all desired range (100 m to 4 km). This lens is mounted on an aluminum rail with a fiber holder that houses the optical fiber. A 6″ mirror is also mounted on the same rail to steer the laser beam, and the entire setup is mounted on optical table.

2.7 Balanced detector

An InGaAs heterodyne balanced detector with a bandwidth extending from d.c. to 125 MHz is used to retrieve backscattered signals. The benefit of using a balanced detector is to subtract the two optical input signals from each other, which results in the cancelation of common mode noise. This allows for detection of small changes in the signal path from the interfering noise floor. The photo current is converted into voltage through the detector's transimpedance amplifier module. Detector's noise was measured using a spectrum analyzer while no optical signals were applied to its inputs, gain was set to 1×, transimpedance was set to 1.4 kΩ, coupling was set to DC, and spectrum analyzer's frequency resolution was set to 3 MHz. Detector's noise was equal to −83 dBm, which is 1 dB below detector's specification of 3.6 pW $Hz^{-1/2}$. The detector has a non-flat gain response, **Figure 3**, i.e. the gain of the detector varies with the frequency of the input signals.

To correct for this non-flat gain shape, received signals' power spectrum is divided by the power spectrum of detector's output while no signal is present. The measured power when signal is present can be represented as:

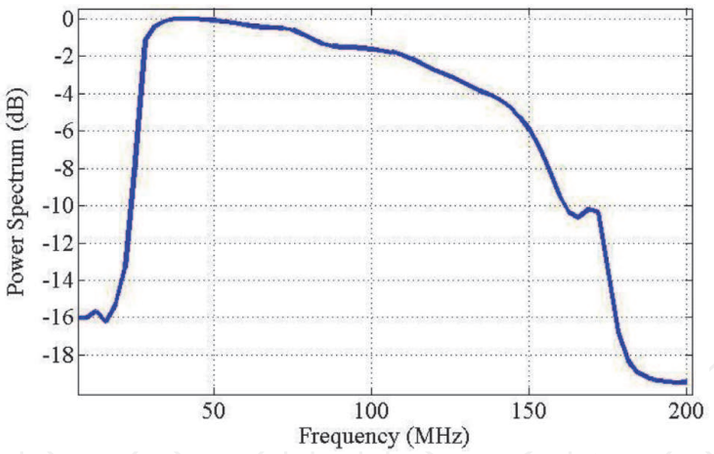

Figure 3.
Non-flat gain response of the heterodyne balanced detector.

$$P_{total} = P_{sig} + P_{noise} \tag{14}$$

Dividing this measured power spectrum by the power spectrum where no signal is present gives:

$$\frac{P_{total}}{P_{noise}} = 1 + \frac{P_{sig}}{P_{noise}} \tag{15}$$

$$= 1 + SNR \tag{16}$$

where SNR: is the signal to noise ratio.

Subtracting 1 from Eq. (16), gives the SNR. The previous technique is used in our signal processing to estimate backscattered signal power.

2.8 Polarized maintained (PM) fiber optic

All optical components are connected through PM optical fibers to ensure that the polarization state of the electric field of the local oscillator and that of the backscattered signals are very close, if not the same. Maintaining the polarization state throughout the different components of the system ensures a high level of the heterodyne detected signals.

3. Power analysis and SNR range dependence

In this section, noise components of the heterodyne photodetector are analyzed, detailed SNR analysis is presented, and the optimum local oscillator power level is determined. The range dependence of SNR is also investigated, and system performance is evaluated. Analytical and experimental wideband SNR was compared. In Section 1, we present the SNR at the heterodyne detection and in Section 2 we present the range dependence of the wideband SNR.

3.1 Transceiver noise analysis

In optical heterodyne detection, The SNR of the Lidar system determines the system's ability to detect low level backscattered signals out of noise [9, 10]. Lidar heterodyne photoreceiver optimization is required to increase the receiving sensitivity [11].

It was shown that heterodyne detection sensitivity can reach its maximum value if local oscillator power is set to an optimum level [10]. The following analysis presents different heterodyne photodetector's noise components and gives an estimate to SNR.

The noise at the output of the optical detector consists of: (1) thermal noise (Johnson noise), (2) shot noise due to local oscillator induced current, and (3) laser's relative intensity noise (RIN).

Thermal noise is related to the detector and does not depend on the local oscillator power (P_{lo}). Thermal noise is expressed as:

$$< i_{th}^2 > = \frac{4kTB}{R_l} \tag{17}$$

where: k is Boltzmann's constant, T is temperature in degrees Kelvin, B is detector's bandwidth, and R_l is detector's load resistor.

Shot noise, unlike signal powers that cancel through the balanced detector, the uncorrelated shot noise adds [12], resulting a mean-square noise at the output of the detector given by:

$$< i_{sh}^2 > = 2eiB \tag{18}$$

where: i is the detector's current caused by the local oscillator power. This current can be calculated as follows:

$$i = en_e \tag{19}$$

where, n_e is the number of electrons, which is given by:

$$n_e = \eta_q e_{ph} \tag{20}$$

where, n_{ph} is the number of photons incident on the detector, η_q is detector's optical efficiency.

$$e_{ph} = \frac{P_{lo}}{h\nu} \tag{21}$$

$$\therefore < i_{sh}^2 > = \frac{2\eta_q e^2 B P_{lo}}{h\nu} \tag{22}$$

Laser relative intensity noise (RIN) is a property of the laser source, which is related to square value of local oscillator power through the following relationship:

$$< i_{RIN}^2 > = (R_{in}) R_b \left(\frac{e\eta_q}{h\upsilon}\right)^2 B(P_{lo})^2 \tag{23}$$

where: R_b is *RIN* suppression ratio through the use of balanced detection. The SNR can now be expressed as:

$$SNR = \frac{< i_s^2 >}{< i_{th}^2 > + < i_{sh}^2 > + < i_{RIN}^2 >} \tag{24}$$

$$= C\left[1 + \frac{2kTh\upsilon}{\eta_q e^2 P_{lo} R_l} + \frac{\eta_q R_{in} R_b P_{lo}}{2h\upsilon}\right]^{-1} \tag{25}$$

where: C is an independent term of local oscillator power $= \frac{\eta_q}{Bh\upsilon} P_s$. When P_{lo} is small, the second term in the denominator of Eqs. (3)–(9) dominates, and *SNR* is

directly proportional to P_{lo}. Hence SNR increases with increasing P_{lo}. On the other hand, when P_{lo} is large, the third term in the denominator dominates, and *SNR* is inversely proportional to P_{lo}. The *SNR* then decreases with increasing P_{lo}. This means that *SNR* will increase as local oscillator power increases until it reaches a maximum value (where P_{lo} is optimum), after which it starts to decrease. The optimum value of P_{lo} can be determined by plotting the SNR as a function of P_{lo} assuming room temperature, $R_{in} = -152$ dB as provided by our laser vendor, $R_b = -25$ dB, $\eta_q = 0.8$, and $R_l = 50\ \Omega$. It is shown that *SNR* is maximum when P_{lo} is approximately = 10 mW, however, we chose to set P_{lo} to approximately 5 mW to avoid operating the detector near its damage threshold, **Figure 4**.

3.2 Coherent Lidar signal range dependence

In this section, we study the range dependence of SNR for the coherent laser radar (CLR) heterodyne detection using a mono-static configuration, and we compare analytical and experimental results. Mono-static configuration was believed to have an improved performance due to the correlation of the transmitted and back scattered fields. This correlation is the result of wave-front tilts self correction in a mono-static configuration [13–15]. The SNR range dependence of a CLR mono-static system is evaluated by using the concept of backprojected local oscillator (BPLO), which is the imaginary local oscillator field distribution projected at the target side of the receiver aperture, receiver lens, originating from the detector [13, 16, 17]. Frehlich and Kavaya [13] derived an equation that describes SNR as a function of range assuming a Gaussian Lidar system i.e., transmitter and LO fields are deterministic, detector response function is uniform, and the detector collects all LO and backscattered power incident on the receiver aperture. The SNR was then found by calculating the overlap integral between the BPLO and the backscattered fields on the receiver plane assuming a distributed aerosol target assuming ideal conditions, i.e. shot noise limited detector and a deterministic beam. To take into account the effects of refractive turbulence on CLR performance, different techniques of wave propagation in random medium were used [18]. Analysis shows that the SNR is proportional to the product of direct detection power and heterodyne efficiency. The calculation of received power and SNR requires mutual coherence function of the backscattered field incident on the receiver. As for natural aerosol targets, backscattered field at each aerosol particle has a random phase, and the mutual coherence function of the total backscattered

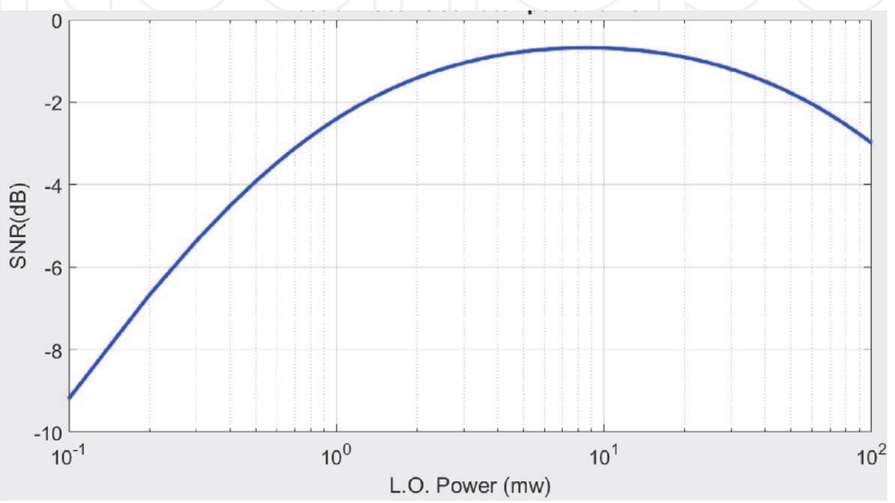

Figure 4.
Normalized SNR *as a function of local oscillator power* P_{lo}.

field is the integration of all mutual coherence functions from each aerosol particle. The SNR range dependence equation is expressed as [19]:

$$SNR(L) = \frac{\eta_D(L)\lambda E\beta K^{2L/1000}\pi D^2}{8hBL^2} \tag{26}$$

where; η_D is the system efficiency, given by:

$$\eta_D(L) = \frac{\eta_{total}}{\left\{1 + \left(1 - \frac{L}{L_F}\right)^2 \left(\frac{\pi(A_C D)^2}{4\lambda L}\right)^2 + \left(\frac{A_C D}{2S_O(L)}\right)^2\right\}} \tag{27}$$

where; the parameters of Eqs. (26) and (27) are introduced in **Table 1**.

The performance of a 4″ diameter antenna was evaluated both theoretically and experimentally while focusing the laser beam at approximately 1.8 km. Continuous 38 range gates having a length of 0.32 μs (48 m range resolution) were obtained between a minimum range of 128 m and a maximum range of approximately 2 km. The power spectra of received signals from 10,000 laser shots were accumulated and wideband SNR was estimated. **Figure 5** shows theoretical and experimental

Parameter	Descriptions	Value
L	Range (m)	
B	Bandwidth	100 MHz
λ	Wave length	1545.2 μm
E	Pulse energy	7 μJ
D	Effective aperture diameter	0.15 m
τ	Pulse width	200 ns
β	Atmospheric backscatter coefficient	8.3×10^{-7} m/sr
K	One way atmospheric transmittance	0.95 km
L_F	Focal range of optical antenna	1.8 km
A_c	Correction factor	0.76
Cn^2	Refractive index structure constant	2×10^{-14} $m^{-2/3}$
η_{total}	Total system efficiency	−2.2 dB
$S_o(L)$	Transverse coherent length	$\sim(1.1\, kw^2 L\, Cn^2)^{-3/5}$
kw	Wave number = 2π/λ	

Table 1.
Parameters corresponding to analytical estimation of wideband SNR range dependence.

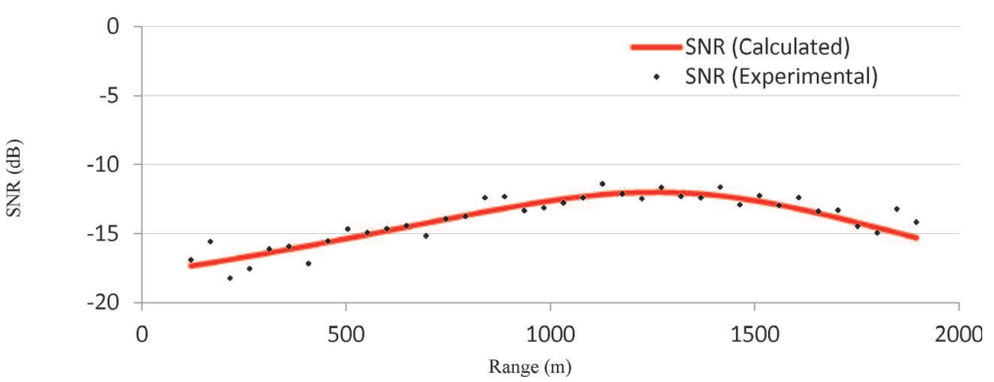

Figure 5.
Wideband SNR range dependence (points, experimental; solid curve, theoretical).

wideband SNR range dependence. It is clear that both measured and theoretically calculated wideband SNR have a very good agreement. The parameters used in this analysis are listed in **Table 1**.

4. FPGA programming and wind measurements analyzed using FFT

For a 20 kHz PFR and a 14-bit ADC with a sampling rate of 400 MHz, data transfer rate from the data acquisition card to the host PC will be 800 Mbyte/s. This high data transfer rate is difficult to be achieved and requires additional hardware and software. Moreover, the amount of data collected in 1 day will be more than 69 Tbyte, which makes data archiving for just a few days nearly impossible. Due to the fast PFR, signal processing on the host computer cannot be achieved in real time, and will cause data to be lost. Therefore, programming the FPGA to calculate power spectra or correlograms of backscattered signals and accumulate the results over a large number of pulses (we chose 10 K pulses) will not only take the burden off the host PC and allow for real time analysis, but will significantly reduce data transfer rate across the PCI express bus to the host PC. In this approach, a signal processing algorithm is implemented and programmed onto the FPGA so that backscattered signals time gating, power spectrum calculation, and accumulation will all be simultaneously carried out on the hardware level as soon as signals are acquired by the ADC. Power spectrum of backscattered signals can be estimated directly by calculating the FFT of the time gated signals, or by calculating the FFT of signals' autocorrelation. FFT pre-processing algorithm and wind measurement results using FFT technique will be explained in the following sections, while autocorrelation pre-processing algorithm and wind measurement results using autocorrelation technique will be explained in details in Section 5.

4.1 ADC card

Backscattered signals are sampled at 400 MSPS using a 14-bit ADC card, which features two 14-bit, 400 MSPS A/D and two 16-bit, 500 MSPS DAC channels with a Virtex5 FPGA computing core and a PCI Express host interface. The Virtex5 FPGA can be programmed using VHDL and MATLAB using the Frame Work Logic toolset. The MATLAB Board Support Package (BSP) allows for real-time hardware-in-the-loop development using graphical, block diagram Simulink environment with Xilinx System Generator toolset. Software tools for host PC development can be performed using C++.

4.2 FPGA programming algorithms

A signal pre-processing algorithm is initially implemented as a logic design, which can be simulated and tested using Matlab/Simulink software. This logic design is then compiled using Xilinx system generator toolset to produce a hardware VLSI image, which can be downloaded into the FPGA. We chose to pre-process backscattered signals in two different techniques: (a) calculate the FFT of time gated signals then accumulate the resulting power spectrum, and (b) calculate the autocorrelation of the backscattered signals then accumulate the resulting autocorrelation matrix for 10 k laser shots.

4.3 FFT pre-processing algorithm

In this pre-processing algorithm, received signals are time gated into portions corresponding to spatial range gates, FFT is estimated for each range gate, and the

corresponding power spectra are accumulated over 10 k laser shots. Power spectrum can be calculated using the FFT as follows:

The normalized Fourier transform of a time domain signals $f(t)$ can be expressed as:

$$F_T(w) = \frac{1}{\sqrt{T}} \int_0^T f(t)\, e^{-iwt}\, dt \tag{28}$$

The discrete spectral density can then be found as:

$$PSD(w) = \lim_{T \to \infty} E\left[\left|F_T(w)^2\right|\right] \tag{29}$$

Eq. (29) shows that the squared modulus of the Fourier transform is the power spectrum. Therefore, we program the FPGA to calculate the square modulus of the output of the FFT block. Our ADC vendor provided us with an FPGA logic design that streams digitally converted signals (sampled at 400 MHz rate) across the PCI express bus to the host PC. This logic design accepts an external trigger signal to start data acquisition. A 20 kHz signal synchronized with laser pulses is used to trigger the data acquisition process. The ADC card operates in a frame mode in which it acquires a frame of incoming data every time it receives an external trigger's interrupt. A frame size of 8192 samples is chosen, which corresponds to approximately 3.1 km. Xilinx Fast Fourier Transform 7.1 circuit block is used in a pipelined-streaming-io mode to calculate FFT for a vector of 128 samples of time gated scattered signals (corresponding to a 48 m spatial resolution). Logic circuits that calculate the modules of the FFT complex output are also implemented and integrated with this design.

4.4 Host computer signal processing

Once accumulated power spectra are streamed from the FPGA across the PCI express bus, data post processing is carried out on the host PC to estimate various parameters such as radial wind velocity, backscattered signal strength, and velocity statistics. Data archiving and visualization are also carried out on the host PC.

The Doppler lidar estimate of the radial component v (m.s^{-1}) of the velocity vector is obtained from the mean-frequency Δf (Hz) of the Doppler lidar signal as:

$$v = \frac{\lambda}{2} \Delta f \tag{30}$$

where λ (m) is the laser wavelength. As a result, the maximum radial velocity that can be measured is given by:

$$v_{max} = \frac{\lambda}{2} f_{\max}, \tag{31}$$

which is approximately 30 m s^{-1}.

The main parameter of interest in Doppler wind measurement is the mean frequency shift of the backscattered signal, because it is directly proportional to the mean velocity of moving aerosol particles within the atmosphere [20, 21]. Doppler frequency shift can be estimated by finding the centroid of the discrete power spectrum of the backscattered signal after removing the amplifier gain shape [22]. One easily calculated method of finding this frequency from a discrete power spectrum is to find the frequency of the highest power, i.e. the frequency

corresponding to the peak power [23]. If the backscattered signal's mean frequency shift and the frequency corresponding to the peak power do not coincide, the velocity estimate can be off by as much as one-half of a frequency resolution.

4.5 Setup procedure to observe scattered signals

Initially the following procedure was followed when measurements were taken at the remote sensing laboratory of the CCNY to assure the fiber's optimum alignment with respect to the lens. In this procedure, the laser pulses were shot at a hard target (~100 m), and the scattered signal was obtained and monitored on the oscilloscope. **Figure 6** shows the scattered signal off a hard target in time domain. Maximizing the magnitude of the hard target's scattered signal through adjusting fiber's x, y, and z positions achieves the optimum fiber's location to focus the beam at about 100 m (the hard target's distance). To focus the beam at a different distance, the z position of the fiber holder can be adjusted accordingly. We then direct the laser beam away from the hard target to obtain atmospheric backscattering, **Figure 7.**

4.6 Real-time wind measurement

In this section, real-time wind measurements are reported. Real-time measurements are recoded continuously, thanks to FPGA pre-processing techniques that allow for streaming of either power spectrum or autocorrelation of received signals instead of raw data. The instrument was installed in our research vehicle that is located at the City College of New York at upper Manhattan, New York (latitude: 40.49°N, longitude: 73.56°W). Laser pulses are transmitted into the atmosphere through an opening in the vehicle's roof, **Figure 8**. The following subsections introduce vertical wind velocity measurements using FFT and autocorrelation pre-processing techniques. Horizontal wind speed measurement is also introduced.

4.7 Vertical wind velocity measurement using FFT pre-processing algorithm

Received signals are pre-processed on the FPGA by dividing backscattered signals into 128 samples per a range gate, corresponding to a 48 m range resolution,

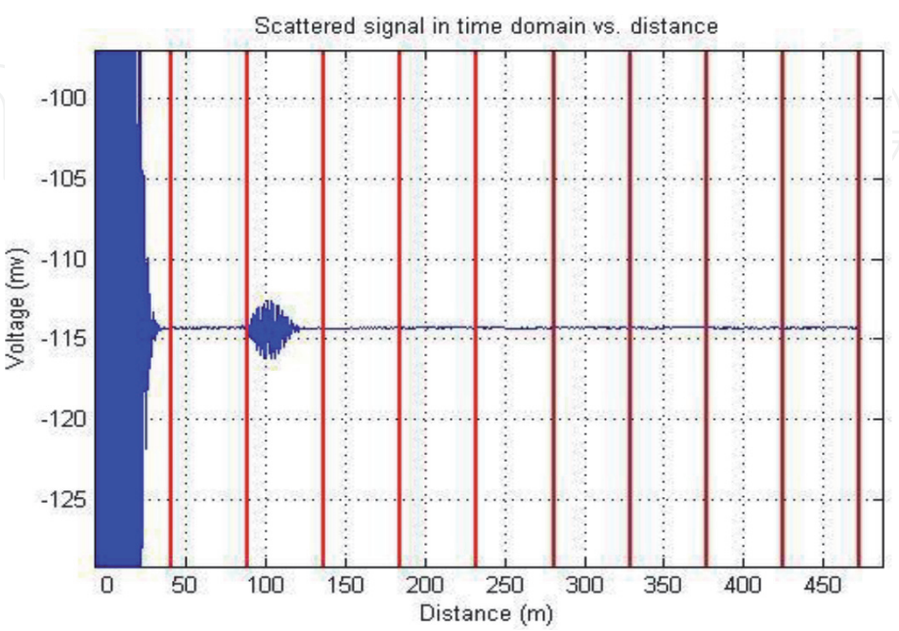

Figure 6.
Time domain scattered signal off a hard target.

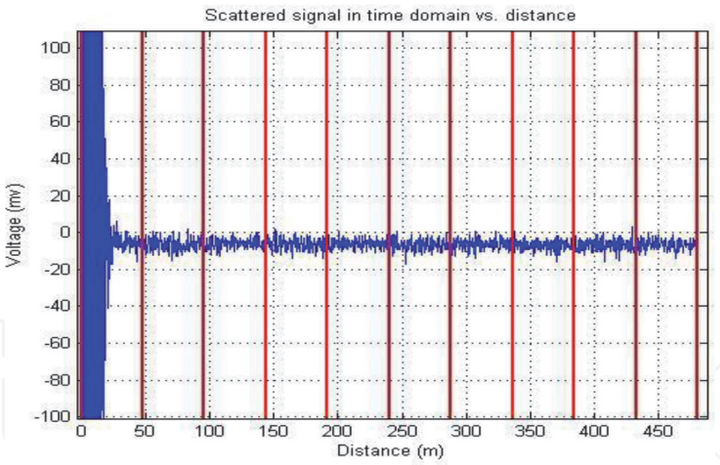

Figure 7.
Time domain scattered signal off the atmosphere.

Figure 8.
The research van where the Doppler lidar instrument is installed for field measurements.

ranging from 96 m to approximately 3 km. Power spectra of the gated signals are estimated by calculating the FFT and then accumulating the resulted power spectrum for 10,000 shots. Accumulated power spectra are streamed to the host PC for further processing and archiving. Wind velocities are calculated by estimating the Doppler frequency shift of the received signals' power spectrum. Three different techniques are used for velocity estimate; spectral peak search, power spectrum peak curve fitting, and MLE algorithm.

In the following section, vertical measurement results of wind velocity measured during the month of August of 2011 are introduced and discussed. The vertical wind velocity profile was measured on August 17th, 2011 from 14:35-to-16:35 EDT. Scattered signals' power spectrum is flattened by dividing it by the power spectrum of input signals to the photo-detector when no scattered signals are present. A signal intensity threshold is chosen below which any returned signals power spectrum is ignored. In **Figure 9**, vertical wind velocity is estimated by fitting the power spectrum profile around the peak value to a Gaussian curve shape and finding the centroid of the fitted shape. It is also shown that updrafts and downdrafts are very visible, which is typical weather condition during a summer afternoon.

Backscattered signals' power was estimated by integrating the area under the power spectrum curve, **Figure 10**. The signal power was then range corrected by dividing estimated power by the overlap integral function given that the laser beam was focused at a known distance (approximately 2 km), which was determined by scattering off a hard target (clouds).

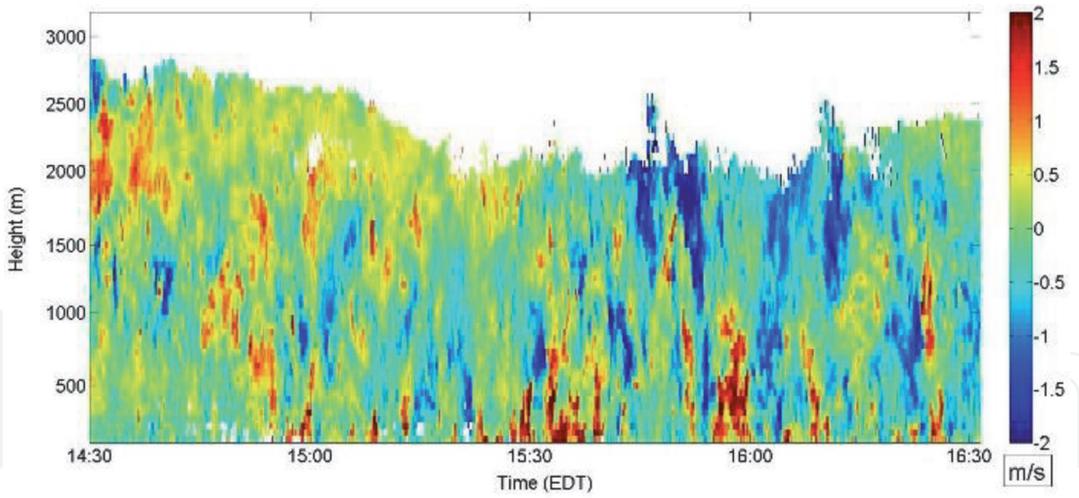

Figure 9.
Vertical wind velocity profile (m/s) measured at CCNY on August, 17th, 2011 from 14:35–16:35 PM EDT estimated by Gaussian curve fitting.

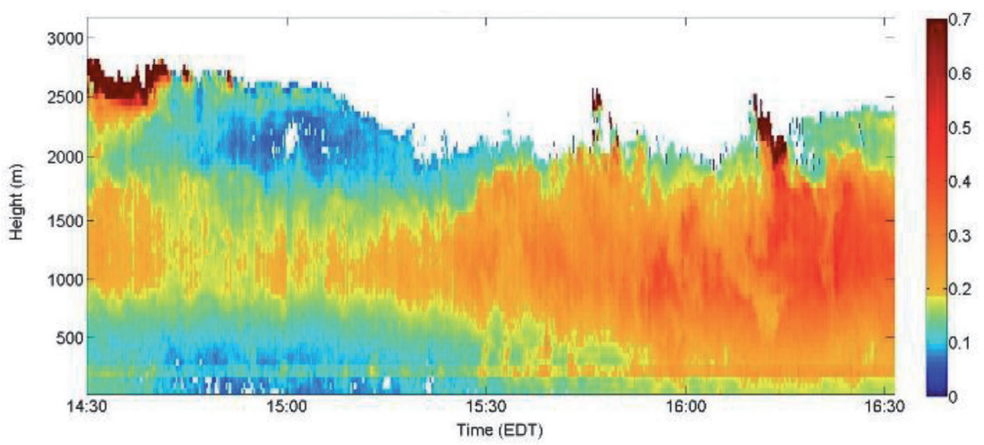

Figure 10.
Ratio of received signals power to shot noise power V.s. time and height measured at CCNY on August, 17th, 2011 from 14:35–16:35 PM EDT.

Range correcting received signals' power allows for comparison our results with the results of a 1 μm direct detection lidar, which was operated at the remote sensing laboratory of the City College of New York during the same time of operation. **Figure 11A** and **B** show a good agreement of signal intensity profile's and cloud patterns with that of the CDL at 14:30, 15:50 and 16:15. It is also noticed that signal intensity increased significantly at a height of approximately 2700 m at 14:30 and 16:20 due to clouds at that height. Both lidars also show a gradual increase of aerosol concentration as a function of time between 16:00 and 16:30. The Doppler lidar's signals power spectrum comparison with the direct detection measurements proves that the obtained power spectrum is valid, and as a result, the frequency shift has to be due to: (a) RF signals going into the AOMs, and (b) Doppler shift caused by wind. Since the LO is stable (laser's line width is approximately 3 kHz), and the jitter between the RF signal and the ADC's clock is less than 100 kHz, then measured frequency shifts are solely due to Doppler shifts caused by wind velocity.

As mentioned in Section 2, the power spectrum of received signals needs to be corrected for the detector's non-flat gain shape. This is done by dividing the power spectrum of received signals by a power spectrum of reference signals. The reference signals are obtained using the detector while LO is turned on and no received signals are present (final amplifier is turned off), i.e. this power spectrum only represents shot noise. The SNR can be represented as follows:

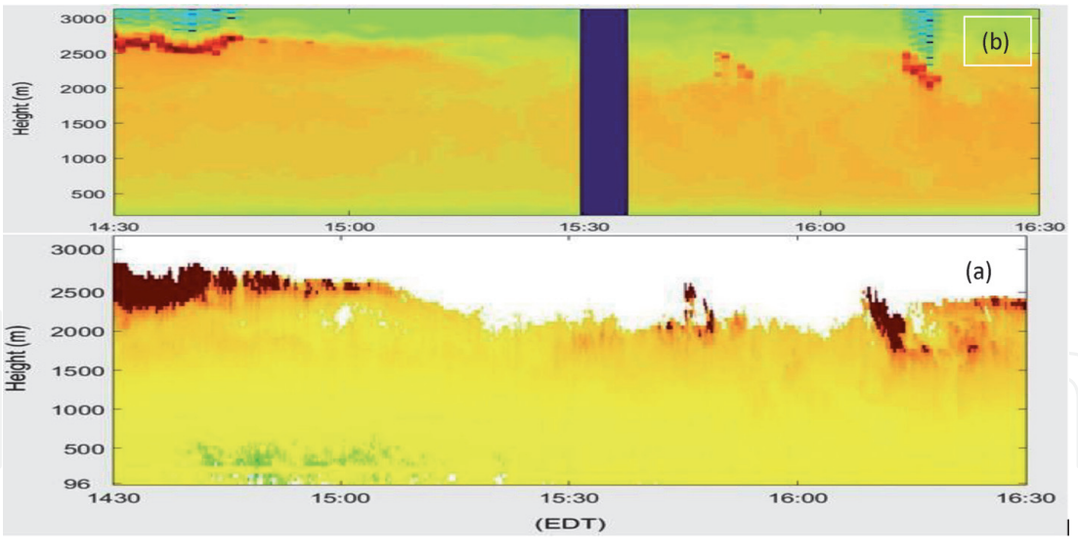

Figure 11.
Range corrected backscattered signal power V.s. time and height (a) and the 1 μm direct detection lidar signal power vs. height and time (b). Both signals power profiles show a good agreement around 14:35, 15:60, and 16:15, where clouds' patterns are observed at the same heights. Aerosols concentration profiles also show a good agreement in the two measurements.

$$SNR = \frac{P_{sig}^{(N)}}{P_{nois}} \tag{32}$$

where, P_{nois}, and $P_{sig}^{(N)}$ are the noise and signal power accumulated over N pulses, respectively. For a shot noise limited receiver system, the noise power is due to shot noise: $P_{shot}^{(N)}$, which can be given by:

$$P_{shot}^{(N)} = < P_{shot} > \pm \sigma_{shot}^{(N)} \tag{33}$$

where; $< P_{shot} >$ is the average shot noise power, which is a fixed level characterized by the laser source, and $\sigma_{shot}^{(N)}$ is the shot noise variation around its fixed level when averaged N times (standard deviation of the shot noise for N accumulation). The average shot noise fixed power level is given by:

$$P_{shot} = 2eiB \tag{34}$$

where; e is the electronic charge, i is the photo-current, and B is the detector's bandwidth.

In our analysis, we calculate the following parameter: $\frac{P_{measured}}{P_{ref}} - 1$ by dividing signals power spectrum by a reference signals power spectrum and then subtracting one, which results to:

$$\frac{P_{measured}}{P_{ref}} - 1 = \frac{(SNR)}{\sqrt{N}} + \sqrt{\frac{2}{N}} \tag{35}$$

Therefore, when accumulating 10,000 pulses and in order to extract signal out of noise, the signal power should be at least equal to noise power, i.e. SNR =1. As a result, the value we calculate is equal to: $\frac{1}{\sqrt{10,000}} + \frac{\sqrt{2}}{\sqrt{10,000}} = 0.024$, which is the value we set as a threshold below which received signals are ignored. It is also worth noting that the signal power we report is not really the signal power, but it's the signal power normalized to the shot noise, in other words, it is the SNR for a single shot.

5. FPGA programming and wind measurements analyzed using autocorrelation

The objective of processing received signals using this technique is to have the ability to change the spatial resolution. This is achieved by calculating the autocorrelation of received signals and using it to calculate the power spectrum of any desired range gate [24]. The power spectrum of received signals is found by calculating the FFT of the autocorrelation as shown in Eqs. (36) and (37).

$$R(\tau) = \int_{-\infty}^{\infty} f(t)f(t+\tau)dt \tag{36}$$

$$G(f) = \int_{-\infty}^{\infty} R(\tau)e^{-j2\pi f\tau}\, dt \tag{37}$$

where; $f(t)$ is a time domain signal, $R(\tau)$ is the signal's autocorrelation, and $G(f)$ is the Fourier transform (power spectrum).

Changing range gates (varying spatial resolution) is an advantage that previous FFT pre-processing algorithm does not have. In this technique (autocorrelation), digitized received signals are split into two paths. The first path is mixed with a cosine signal oscillating at 84 MHz to produce an in-phase (I) component; the other path is mixed with a sine signal oscillating at 84 MHz to produce a quadrature (Q) component, **Figure 12**.

5.1 Autocorrelation (analog complex demodulator) pre-processing algorithm

Mixing the received signals (oscillating around 84 MHz +/− Doppler shift) with an 84 MHz cosine and sine waves produces two output signals; a high frequency (sum of the two frequencies) component and low frequency (difference of the two frequencies) component (the Doppler shift). A low-pass, finite impulse response (FIR), filter is used on each path to get rid of the unwanted high frequency. Filtered signals are then down-sampled (decimated) by a factor of 4, which will reduce our original sampling period from 2.5 n.s (400 MHz) to 10 n.s (100 MHz). This down conversion reduces the maximum detectable frequency (according to Nyquest theorem) to 50 MHz, which corresponds to a radial velocity of approximately 38 m/s. The resulting complex time sequence $d(n) = d_i(n) + j\, d_q(n)$ is input to the (M)-lag autocorrelator circuit,

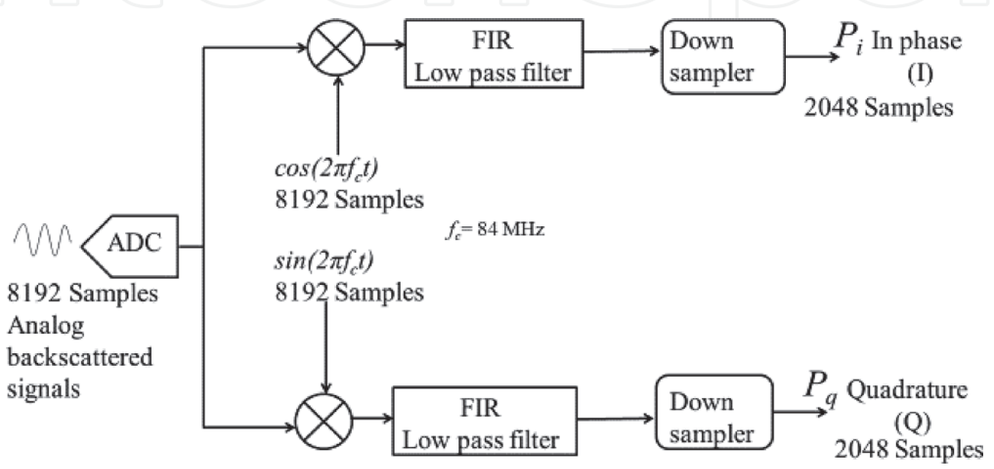

Figure 12.
Autocorrelation algorithm block diagram as implemented on the FPGA to produce an in-phase (I) and a quadrature (Q) signals.

which computes an autocorrelation matrix $D(m,n) = d^*(n).d(n + m)$ for m = 0 to M-1 (lags) and n = 0 to N-1 (number of time domain samples, which is 8k samples/4 = 2 k), where $d^* = d_i(n) - j\, d_q(n)$ is the complex conjugate of $d(n)$. The processing repeats for 10 k laser shots and the elements of D matrix are accumulated and then streamed to an output buffer before it is being streamed to the host PC.

Once the accumulated lags' matrix [Eq. (5)–(3)] is streamed to the host PC, further processing is conducted to calculate the power spectrum of received signals as follows:

$$D = \begin{bmatrix} S_0S_0^* & S_0S_1^* & S_0S_2^* & \dots & \dots & S_0S_{M-1}^* \\ S_1S_1^* & S_1S_2^* & S_1S_3^* & \dots & \dots & \vdots \\ S_2S_2^* & S_2S_3^* & S_2S_4^* & \dots & \dots & \vdots \\ \vdots & \vdots & \vdots & \dots & \dots & \vdots \\ S_{n-1}S_{n-1}^* & S_{n-1}S_{n-2}^* & 0 & \dots & \dots & \vdots \\ S_nS_n^* & 0 & 0 & \dots & \dots & \vdots \end{bmatrix} \quad (38)$$

where; M is the number of lags, n is the number of acquired samples, S denotes to a sample, and S^* denotes to the complex conjugate of sample S.

To calculate the power spectrum of a certain range gate, the columns of the D matrix are accumulated from the i^{th} row to the j^{th} row, where i and j are the first and last corresponding samples of that range gate, respectively. This accumulation process produces an M size autocorrelation vector, which is complex (in-phase and quadrature components). Since the autocorrelation is symmetric, we construct the second half of the autocorrelation vector by making its real part even and imaginary part odd. Finally, we find the power spectrum of that range gate's signals by calculating the FFT of the constructed complex autocorrelation vector.

5.2 Vertical wind velocity measurements using autocorrelation pre-processing algorithm

In this section, wind velocity was measured in a vertical mode while pre-processing received signals using an autocorrelation algorithm. The autocorrelation algorithm calculates the autocorrelation of the received signals and streams out the lags matrix that can be gated according to user's range resolution's preference. That feature makes autocorrelation technique advantageous over the FFT technique, where range gates are fixed. Wind velocity was measured under this mode of operation on July 12th, 2012, **Figure 13**.

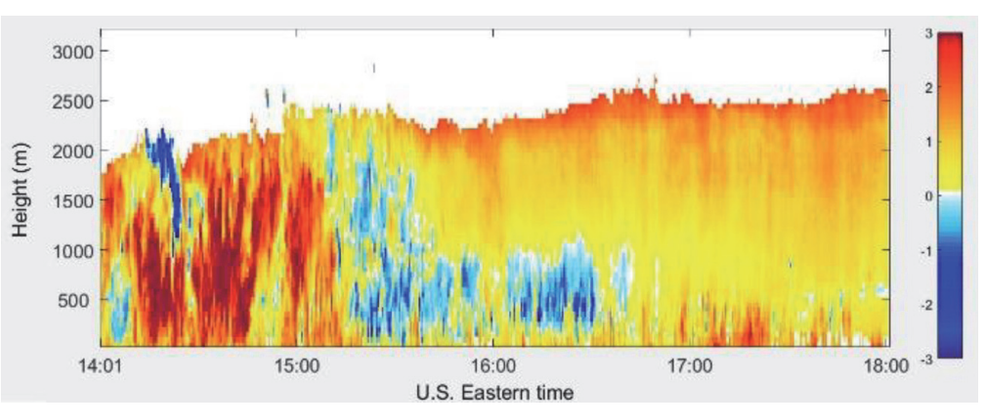

Figure 13.
Vertical wind velocity (m/s) vs. time and height measured at CCNY remote sensing laboratory between 14:01–18:00 PM EDT on July 12th, 2012.

6. Conclusion

In conclusion, an eye-safe all-fiber CDL system for wind sensing in urban areas was designed, developed, tested, and operated at the remote sensing Laboratory of the City College of New York.

The system utilizes a 1.5 μm fiber optics laser, which benefits from the availability and affordability of telecommunication optical components. Two AOMs are connected in series to achieve a high extinction ratio and to shift the laser frequency by 42 MHz each, which produces a total shift of 84 MHz. An optical amplifier amplifies the laser pulse to produce approximately 12 μJ/pulse (200 ns FWHM at 20 kHz PFR). An optical circulator directs amplified laser pulses to its output port that is connected to the optical antenna, and directs received signals to an optical coupler to be mixed with a LO. Circulator's fiber tip was polished and angled to reduce internal reflection that can damage the detector. Optical mixed signals are detected by a heterodyne balanced detector.

Received signals are sampled at 400 MHz through a 14-bit ADC equipped with an FPGA. Due to the very low energy per pulse (12 μJ/pulse), a high PFR (20 kHz) is used to allow for digging the very low signal out of noise. This high pulse rate makes it almost impossible to process the data in real time, therefore, the FPGA was programmed to pre-process received signals at the hardware level as the received signals are being acquired and before streaming to the host PC.

Two different pre-processing algorithms have been simulated and programmed into the FPGA; one algorithm calculates FFT of time gated received signals and accumulates the resulted power spectrum; the other algorithm calculates autocorrelation of the received signals and accumulates the result. The later algorithm allows for changing range gate (spatial resolution), which can be applied to signals scattered from very high altitudes (where signals are very weak) to improve the SNR.

The system was installed in a research vehicle and wind velocity was measured at the City College of New York. Wind velocity was measured in two different modes; vertical mode, and scan mode. Wind velocity was measured up to 3 km in a vertical mode during a very clear day. The system can be operated to measure wind velocity, processes received signals in real time, and display results while acquiring data. Improving the system can be achieved by increasing the measured range to 7 km instead of 3 km.

Author details

Sameh Abdelazim[1*], David Santoro[2], Mark F. Arend[2], Fred Moshary[2] and Sam Ahmed[2]

1 Fairleigh Dickinson University, New Jersey, USA

2 The City College of New York, New York, USA

*Address all correspondence to: azim@fdu.edu

References

[1] Huffaker RM, Jelalian AV, Thompson JAL. Laser-Doppler system for detection of aircraft trailing vortices. IEEE. 1970;**58**:322-326

[2] Kameyama S, Ando T, Asaka K, Hirano Y, Wadaka S. Compact all-fiber pulsed coherent Doppler lidar system for wind sensing. Applied Optics. 2007; **46**:1953-1962

[3] Karlsson CJ, Olsson FÅA, Letalick D, Harris M. Ll-fiber multifunction continuous-wave coherent laser radar at 1.55 νm for range, speed, vibration, and wind measurements. Applied Optics. 2000;**39**:3716-3726

[4] Henderson SW, Suni PJ, Hale CP, Hannon SM, Magee JR, Bruns DL, et al. Coherent laser radar at 2 mm using solid state lasers. IEEE Transactions on Geoscience and Remote Sensing. 1993; **31**:4-15

[5] Kane TJ, Kmetec JD, Wagener TJ. Flight test of 2-mm diode pumped laser radar system. In: SPIE 2464, Air Traffic Control Technologies. Orlando, FL; 1995

[6] Kavaya MJ, Henderson SW, Magee JR, Hale CP, Huffaker RM. Remote wind profiling with a solid-state Nd:YAG coherent lidar system. Optics Letters. 1989;**14**:776-778

[7] Abdelazim S, Santoro D, Arend M, Moshary F, Ahmed S. Development and operational analysis of an all-fiber coherent Doppler lidar system for wind sensing and aerosol profiling. IEEE Transactions on Geoscience and Remote Sensing. 2015;**53**(12):6495-6506

[8] Arend M, Santoro D, Abdelazim S, Gross B, Moshary F, Ahmed S. Development of a NYC Meteorological Network with Emphasis on Vertical Wind Profiles in Support of Meteorological and Dispersion Models. Phoenix, AZ: American Meteorological Society; 2009

[9] Cariou J-P, Augere B, Valla M. Laser source requirements for coherent lidars based on fiber technology. Comptes Rendus Physique. 2006;**7**:213-223

[10] Holmes FJ, Rask BJ. Optimum optical local-oscillator power levels for coherent detection with photodiodes. Applied Optics. 1995;**34**:927-933

[11] Amzajerdian F, Pierrottet D, Singh U, Kavaya M. Optimum integrated heterodyne photoreceiver for coherent lidar applications. MRS. 2005;**883**: PROC-883-FF6.3

[12] Darcie T, Moye A, Driessen P, Bull J, Kato H, Jaeger N. Noise reduction in class-AB microwave-photonic links. Microwave Photonics. 2005;**12**(14): 329-332

[13] Frehlich RG, Kavaya MJ. Coherent laser radar performance for general atmospheric refractive turbulence. Applied Optics. 1991;**30**:5325-5352

[14] Clifford SF, Wandzura S. Monostatic heterodyne lidar performance: The effect of the turbulent atmosphere. Applied Optics. 1981;**20**: 514-516

[15] Wandzura SM. Meaning of quadratic structure functions. Journal of the Optical Society of America. 1980;**70**: 745-747

[16] Kavaya MJ, Menzies RT, Haner DA, Oppenheim UP, Flamant PH. Target reflectance measurements for calibration of lidar atmospheric backscatter. Applied Optics. 1983;**22**: 2619-2628

[17] Yanzeng Z, Post MJ, Hardesty RM. Receiving efficiency of monostatic

pulsed coherent lidars. 2: Applications. Applied Optics. 1990;**29**:4120-4132

[18] Fried DL. Optical heterodyne detection of an atmospherically distorted signal wave front. IEEE. 1967; **55**:57-66

[19] Kameyama S, Ando T, Asaka K, Hirano Y, Wadaka S. Performance of discrete-Fourier-transform-based velocity estimators for a wind-sensing coherent Doppler lidar system in the Kolmogorov turbulence regime. IEEE Transactions on Geoscience and Remote Sensing. 2009;**47**(10):3560-3569

[20] Hardesty RM. Performance of a spectral peak frequency estimator for Doppler wind velocity measurement. IEEE Transactions on Geoscience and Remote Sensing. 1986;**GRS-24**(5): 777-783

[21] Doviak RJ, Zrnic DS. Doppler Radar and Weather Observations. Orlando, FL: Academic; 1984

[22] Hardesty RM. Performance of a discrete spectral peak frequency estimator for Doppler wind velocity measurements. IEEE Transactions on Geoscience and Remote Sensing. 1986; **GE-24**(5):777-783

[23] Sirmans D, Bumgarner B. Numerical comparison of five mean frequency estimators. Meteorological Applications. 1975;**14**:991-1003

[24] Abdelazim S, Santoro D, Arend M, Moshary F, Ahmed S. A hardware implemented autocorrelation technique for estimating power SPectral density for processing signals from a Doppler wind Lidar system. Sensors. 2018;**18** (12):4170. DOI: 10.3390/s18124170